FULL PAPER

Inflammatory Cytokines Presented from Polymer Matrices Differentially Generate and Activate DCs In Situ

Omar A. Ali, Prakriti Tayalia, Dmitry Shvartsman, Sarah Lewin, and David J. Mooney*

During infection, inflammatory cytokines mobilize and activate dendritic cells (DCs), which are essential for efficacious T cell priming and immune responses that clear the infection. Here, macroporous poly(lactide-*co*-glycolide) (PLG) matrices are designed to release the inflammatory cytokines GM-CSF, Flt3L, and CCL20 in order to mimic infection-induced DC recruitment. The ability of these infection mimics to function as cancer vaccines is tested via induction of specific anti-tumor T cell responses. All vaccine systems tested are able to confer specific anti-tumor T cell responses and long-term survival in a therapeutic B16-F10 melanoma model. However, GM-CSF and Flt3L vaccines result in similar survival rates and outperformed CCL20-loaded scaffolds, even though they have differential effects on DC recruitment and generation. GM-CSF signaling is identified as the most potent chemotactic factor for conventional DCs and significantly enhanced surface expression of MHC(II) and CD86(+), which are utilized for priming T cell immunity. In contrast, the use of Flt3L vaccines leads to greater numbers of plasmacytoid DCs, correlating with increased levels of T cell-priming cytokines that amplify T cell responses. These results demonstrate that 3D polymer matrices modified to present inflammatory cytokines may be utilized to effectively mobilize and activate different DC subsets in vivo for immunotherapy.

1. Introduction

Dendritic cells (DCs) orchestrate immune responses to infection and tumors by priming and propagating specific, cytotoxic T lymphocyte (CTL) responses.[1–4] Immature DCs residing in peripheral tissue continuously sample antigens in their environment and are activated by molecular stimuli, such as pathogen associated molecular patterns (PAMPs). DCs are especially adept at processing and presenting antigens on major histocompatibility complexes (MHC), enabling the transmission of antigenic signals to T cells. PAMPs, including lipopolysacharides,

cytosine-guanosine (CpG) sequences in bacterial DNA, or products of dying cells (i.e. danger signals), trigger particular pattern recognition receptors such as toll-like receptors (TLR) that induce DC activation.[1,5,6] Upon activation by danger signaling, DCs upregulate their expression of the costimulatory molecules, CD80 and CD86 along with cytokines that prime T cell responses. Activated DCs then home from sites of infection to the draining lymph nodes (LNs), a process termed lymph node homing, after upregulating CCR7 expression, a chemokine receptor that binds the LN-derived ligands CCL19 and CCL20.[1–6] At the lymph nodes, DCs engage and activate naive T-cells by presenting MHC-antigen complexes with costimulation causing the initiation and expansion of antigen-specific CTLs.[1,5–7]

The ability of particular DCs to initiate and control immune responses is a consequence of both their localization within tissues and their specialized capacity for mobilization.[2] DCs originate from pluripotent stem cells in the bone marrow, enter the blood stream and localize into almost all organs.[1–3] Based on the relative expression of a series of surface markers, different subsets of DCs or DC precursors can be identified in peripheral blood, including plasmacytoid DCs (pDCs) and conventional DCs (cDCs).[2] pDCs are major type I interferon (IFN) producers, and specialize in activating adaptive immune responses to virus challenge via cytokine signaling.[3] CD11c(+) cDCs, such as epidermal DCs, are especially adept at antigen presentation and co-stimulation of T cells.

Upon pathogenic infection and inflammation, DCs rapidly migrate into the draining lymph nodes and primary sites of infection at rates that vastly outnumber other antigen presenting cells, such as macrophages.[4] The production of most DC subsets, including (pDCs) is controlled in the steady state by the cytokine Fms-related tyrosine kinase 3 ligand (Flt3L). Other cytokines, such asgranulocyte macrophage-colony stimulating factor (GM-CSF) and chemokine (C-C motif) ligand 20 (CCL20), released by damaged or infected cells, actively recruit and localize cDCs to the sites of inflammation.[2–4] In inflammatory models, both in vivo and in vitro, these inflammatory cytokines have been shown to also enhance DC migration and proliferation and may regulate the DC activation state.[6,8–13] The

O. A. Ali, P. Tayalia, D. Shvartsman, S. Lewin,
Prof. D. J. Mooney[†]
Wyss Institute for Biologically Inspired Engineering
Harvard University, Boston, MA
E-mail: mooneyd@seas.harvard.edu
P. Tayalia, D. Shvartsman, Prof. D. J. Mooney
School of Engineering and Applied Sciences
Harvard University, Cambridge, MA
[†]Present Address: Harvard School of Engineering and Applied Sciences
29 Oxford St., 319 Pierce Hall Harvard University Cambridge, MA 02138

ADVANCED
FUNCTIONAL
MATERIALS
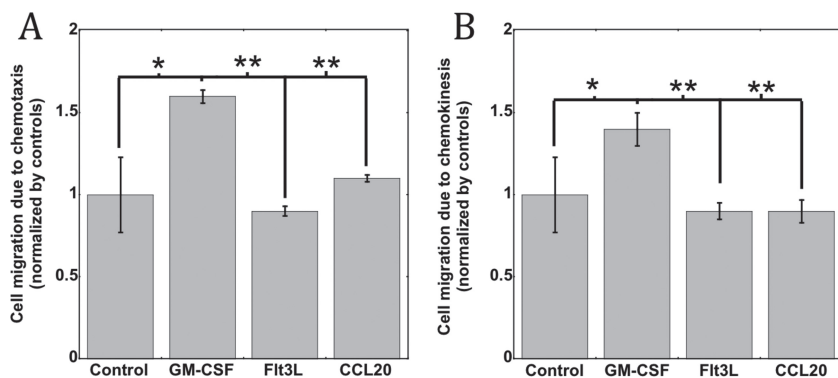www.afm-journal.de

Materials
Views
www.MaterialsViews.com

Figure 1. In vitro chemotaxis and chemokinesis of DCs. The in vitro (A) chemotaxis and (B) chemokinesis of bone marrow derived DCs in response to control media and media supplemented with GM-CSF, Flt3L, and CCL20. *$P < 0.05$ **$P < 0.01$, as compared to GM-CSF loaded matrices. Values represent mean and standard deviation. (n = 4).

observed, as GM-CSF exposure promoted a similar 50% increase in the number of migrated cells in response to homogenous levels of the cytokine (Figure 1B). In contrast, Flt3L and CCL20 had no effect on the chemotaxis or chemokineses of DCs in these assays (Figure 1). These results suggest that GM-CSF has a superior effect on DC mobilization and recruitment in comparison to Flt3L and CCL20.

2.2. Controlled Release of Cytokines and In vivo DC Recruitment

Macroporous, polylactide-*co*-glycolide (PLG) matrices were designed to provide long-term and sustained release of GM-CSF, Flt3L, and CCL20 (Figure 1A) and to house DCs for activation. These PLG scaffolds were 80–90% porous with an average pore size between 125–200 um to facilitate dendritic cell infiltration. The in vitro release kinetics for the three cytokines were similar, as the matrices quickly released protein with a burst over the first 5 days followed by sustained release over the next several weeks (**Figure 2**A). The scaffolds released approximately 43, 36, and 26% of the incorporated GM-CSF, Flt3L, and CCL20, respectively, over the first 4 days followed by approximately 0.9% daily release of protein over the next 23 days (Figure 2A).

To examine the ability of cytokine-loaded, PLG matrices to recruit and activate DCs in vivo, PLG matrices delivering GM-CSF, Flt3L and CCL20 were implanted subcutaneously into the backs of C57BL/6J mice and removed at day 7 after implantation. Immunohistochemical analysis revealed intense CD11c(+) DC infiltrates penetrating the porous network of all the scaffolds releasing cytokines, and GM-CSF mediated the most dense DC clustering (Figure 2B). The magnitude of DC infiltration and activation into the matrices was quantified by FACS analysis of cell populations isolated from the polymeric material. Blank PLG matrices recruited approximately 190 000 CD11c(+) DCs, whereas scaffolds delivering GM-CSF recruited approximately 960 000 DCs, equating to over a 5-fold difference in cell recruitment (Figure 2C). Scaffolds presenting Flt3L and CCL20 recruited 2.5 fold more DCs than control conditions, but significantly less than GM-CSF presenting scaffolds (Figure 2C). These results are consistent with the in vitro results that identified GM-CSF as the most potent mobilizing and chemotactic factor for DCs, in comparison to Flt3L and CCL20.

quantity of DCs activated during infection or within tumors is correlated with the strength of the subsequent immune response and disease prognosis.

Because DCs are potent inducers of immunity they are often utilized as platforms for cell-based cancer immunotherapy.[1] To generate sufficient numbers of dendritic cells (DCs) for immunotherapy, laboratory-based culture of DC precursors with inflammatory cytokines, such as GM-CSF and Flt3L has often been used.[14] DCs modified in vitro to present tumor antigens are capable of eliciting antitumor effects in murine models upon transplantation. Initial clinical testing of ex vivo, DC-based vaccines has revealed the induction of tumor regression in a subset of cancer patients, but little survival benefit.[1,15] Protocols involving the ex vivo manipulation of DCs are limited by the quantities and types of DCs that can be produced, poor engraftment efficiency and LN homing, and loss of DC activation upon injection in the in vivo environment.[1–5,16]

To address these limitations, we have developed infection-mimicking materials to present inflammatory cytokines in combination with a danger signal to recruit and activate DCs in vivo.[17,18] Here we compare and contrast the abilities of multiple inflammatory cytokines, GM-CSF, Flt3L, and CCL20 to recruit and activate DCs when delivered from macroporous, implantable polymer scaffolds. We also immobilized nanoparticles containing cytosine-guanosine (CpG) rich oligonucleotide (CpG-ODN) sequences onto scaffolds, as CpG-ODN are expressed in bacterial DNA, and are potent danger signals that can stimulate activation of matrix resident DCs.[17] Finally we tested the ability of these systems to prime anti-tumor T cell responses and confer tumor protection via presentation of cancer antigens.

2. Results

2.1. In vitro Chemotaxis and Chemokinesis of Cytokines

In vitro transwell studies were first conducted to investigate the chemotaxis and chemokinesis effects of bone-marrow derived DCs in response to GM-CSF, Flt3L, and CCL20. GM-CSF gradients promoted significant DC chemotaxis, as DC migration in this condition was approximately 50% higher than the control condition (**Figure 1**A). Similar effects on chemokinesis were

2.3. In vivo DC Activation

PLG scaffolds were modified to present nanoparticles containing TLR-activating, CpG-ODN, as an infection-mimicking danger signal in concert with delivery with inflammatory cytokines. This dramatically enhanced DC activation in situ over control conditions lacking cytokine signaling (**Figure 3**A). Analysis of the activation state of matrix-resident DCs revealed that GM-CSF induced recruitment in combination with CpG-ODN produced significant percentages of activated DCs, as
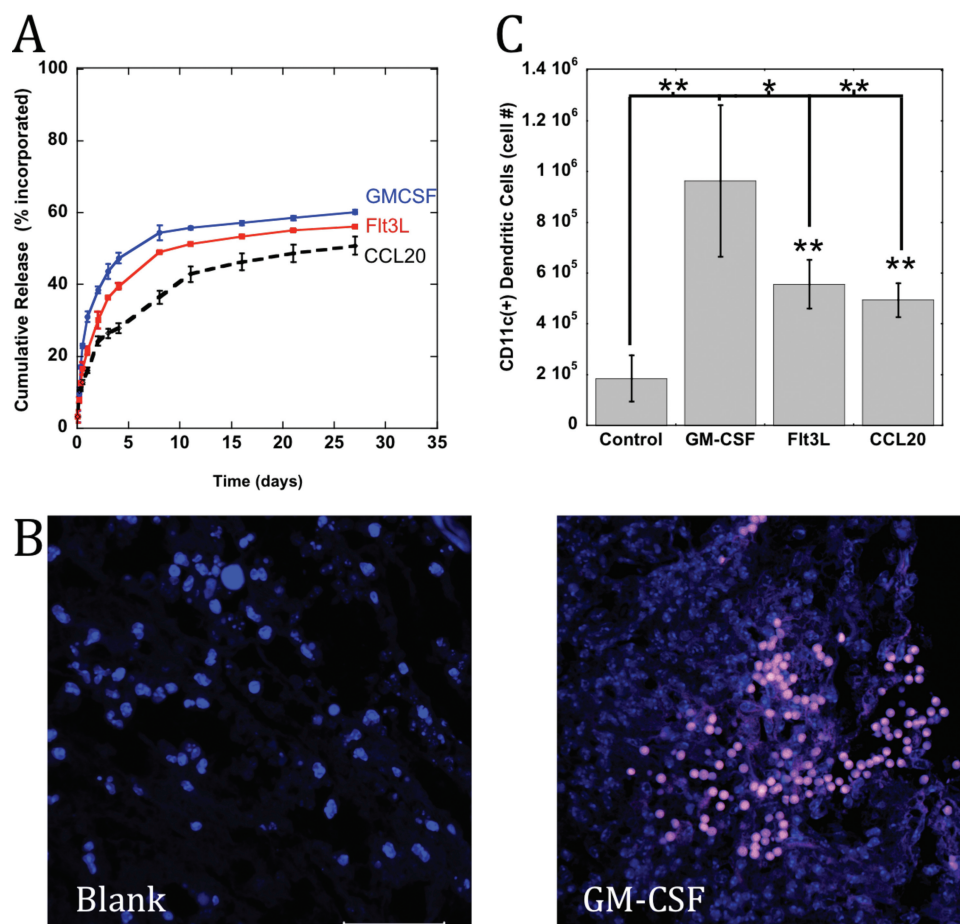
Materials
Views
www.MaterialsViews.com

ADVANCED
FUNCTIONAL
MATERIALS
www.afm-journal.de

FULL PAPER

Figure 2. PLG scaffolds that release cytokines for DC recruitment. (A) The cumulative release of GM-CSF, Flt3L, or CCL20 from PLG scaffolds. (B) Representative photograph of scaffold histological sections stained for CD11c(+) DC infiltrates (pink) into macroporous blank (left) and GM-CSF loaded scaffolds (right) at Day 10 after implantation. Scale bar – 100 um. (C) The total numbers of CD11c(+) DCs at scaffold site at day 7 after implantation of Blank PLG matrices (Con) and matrices loaded with GM-CSF, Flt3L and CCL20. Values represent mean and standard deviations (n = 6). *$P < 0.05$ **$P < 0.01$, as compared to GM-CSF loaded matrices.

MHCII(+) and CD86(+) DCs comprised approximately 54–66% of the total DCs recruited to scaffolds. Approximately 8-fold, 4-fold, and 4-fold increases in the total number of activated DCs were induced by matrices containing GM-CSF, Flt3L, and CCL20, respectively, in comparison to matrices devoid of cytokines (Figure 3B).

Interestingly, Flt3L presentation in combination with CpG-ODN enriched the PLG matrix with the highest average number of CD11c(+)PDCA-1(+) pDCs (Figure 1C), generating over 160,000 resident pDCs. Strikingly, approximately 22% of the total cells in these scaffolds consisted of this DC subset (Figure 3A). This result is in agreement with previous results indicating that Flt3L is a strong mobilizing agent for pDCs.[13] Scaffolds presenting GM-CSF and CCL20 also significantly enhanced pDC generation, leading to approximately 110 000 resident pDCs. The pDC subset has been associated with the induction of t-helper 1 (Th1) immunity via its capacity to induce IL-12 and type-1 interferons (IFNs), which are critical to propagating CTL responses to infections and tumors.[2,7,13] These data indicate that while the three cytokines tested all enhanced DC recruitment and activation, GM-CSF signaling in combination with CpG-ODN produced the highest numbers of activated cDCs, while Flt3L led to the greatest number of resident pDCs.

2.4. Induction of T Cell Immunity and Therapeutic Vaccination

Since infection-mimicking PLG matrices were capable of generating activated DC populations in situ, it was hypothesized that they would induce cytotoxic T-cell responses when utilized as a vaccine. As described previously, B16-F10 tumor lysates were incorporated into PLG matrices as tumor antigens.[17,18] IL-12 and IFN-γ secretion by activated DCs can prime CTL-mediated immune responses and tumor cell death, leading us to quantify the presence of these Th-1 inducers at the scaffold implant site. PLG vaccines presenting Flt3L in combination with CpG-ODN enhanced the local concentration of IL-12 and IFN-γ by 8 and 13-fold, respectively, over control scaffolds (**Figure** 4A and B). GM-CSF release resulted in approximately 3 and 6-fold increases in the local concentration of IL-12 and IFN-γ (Figure 4A and B). CCL20 release from PLG vaccines
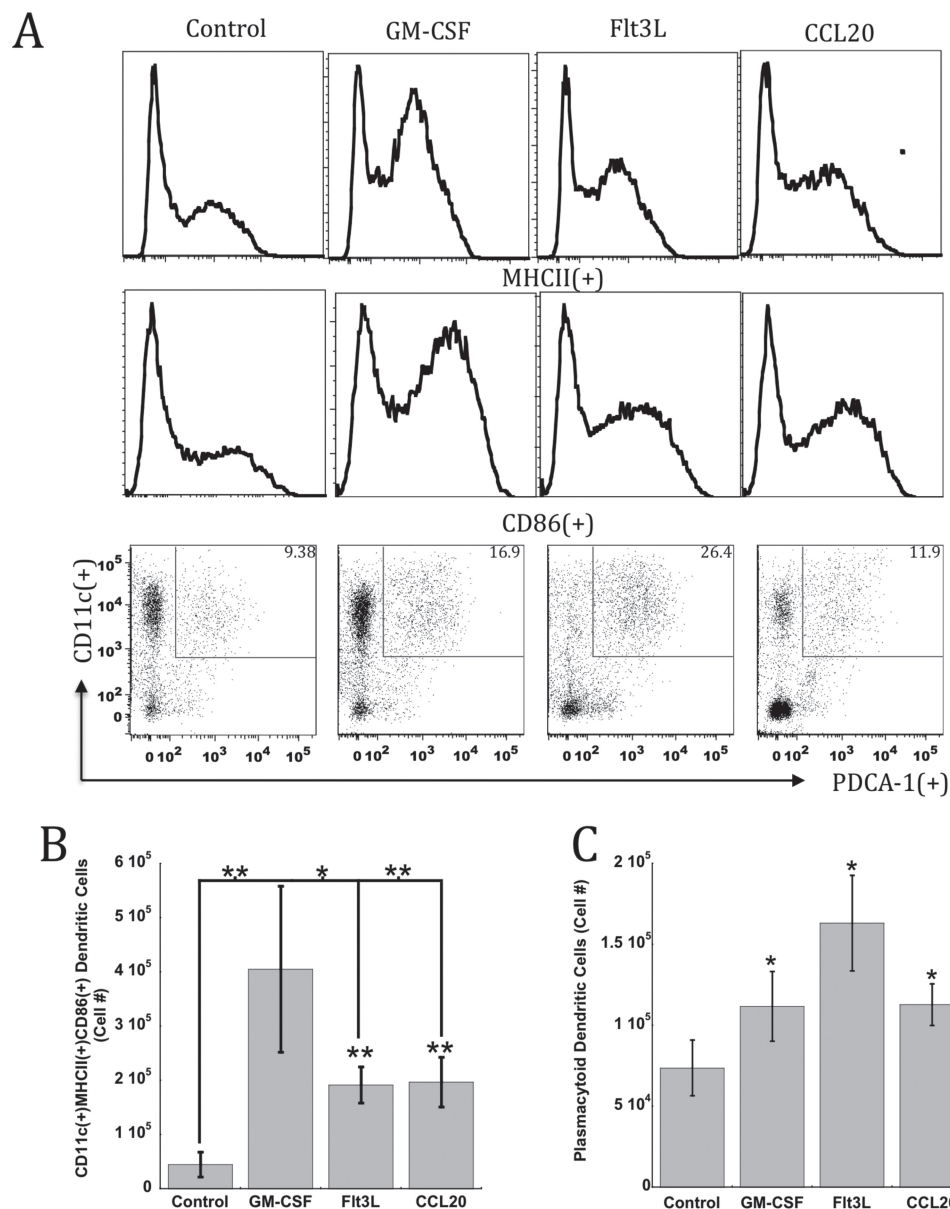
ADVANCED
FUNCTIONAL
MATERIALS
www.afm-journal.de

Materials
Views
www.MaterialsViews.com

Figure 3. DC recruitment and activation mediated by PLG matrices loaded with cytokines and CpG-ODN. (A) FACS histograms and plots representing scaffold infiltrating DCs in CpG-ODN loaded PLG scaffolds (Con) or scaffolds loaded with GM-CSF, Flt3L or CCL20 in combination with CpG-ODN at day 7 post-implantation in mice. Histograms indicate the relative frequency of MHCII and CD86 expression in CD11c(+) DCs infiltrating the indicated scaffold formulation. Dot plots indicate cells stained for CD11c(+) in combination with activated, plasmacytoid DC marker, PDCA-1. Numbers in the upper right quadrant of FACS plots indicate the percentage of CD11c(+)PDCA-1(+) pDCs. (B) The total numbers of activated CD11c(+) DCs positive for MHCII and CD86 expression, and (C) CD11c(+)PDCA-1(+) pDCs present in scaffold at day 7 after implantation of CpG-ODN loaded PLG scaffolds (Con) or scaffolds loaded with GM-CSF, Flt3L, or CCL20 in combination with CpG-ODN. Values represent mean and standard deviations (n = 5). *$P < 0.05$ **$P < 0.01$, as compared to controls (Con) unless otherwise indicated.

led to a 2-fold increase in IL-12 concentration, and no effect on IFN-γ levels at the vaccine site (Figure 4A and B).

The activation of systemic CTL responses was monitored by staining isolated splenocytes with MHC class I/Trp2 peptide pentamers. This allows one to identify CTLs with specificity to tyrosinase-related protein (Trp)-2, which is a main antigenic target of melanoma vaccines in mice and humans. A significant expansion of Trp2 specific CTLs was observed

in the spleens of mice vaccinated with scaffolds incorporating all three cytokines (Figure 4C). Vaccines incorporating Flt3L and GM-CSF led to approximately 5 and 4-fold higher numbers of Trp2 specific CTLs than control vaccines, which was a significantly greater than the T cell response induced by CCL20 vaccines (Figure 4C). Taken together, these data indicate that vaccine formulations containing various inflammatory agents are capable of producing significant and
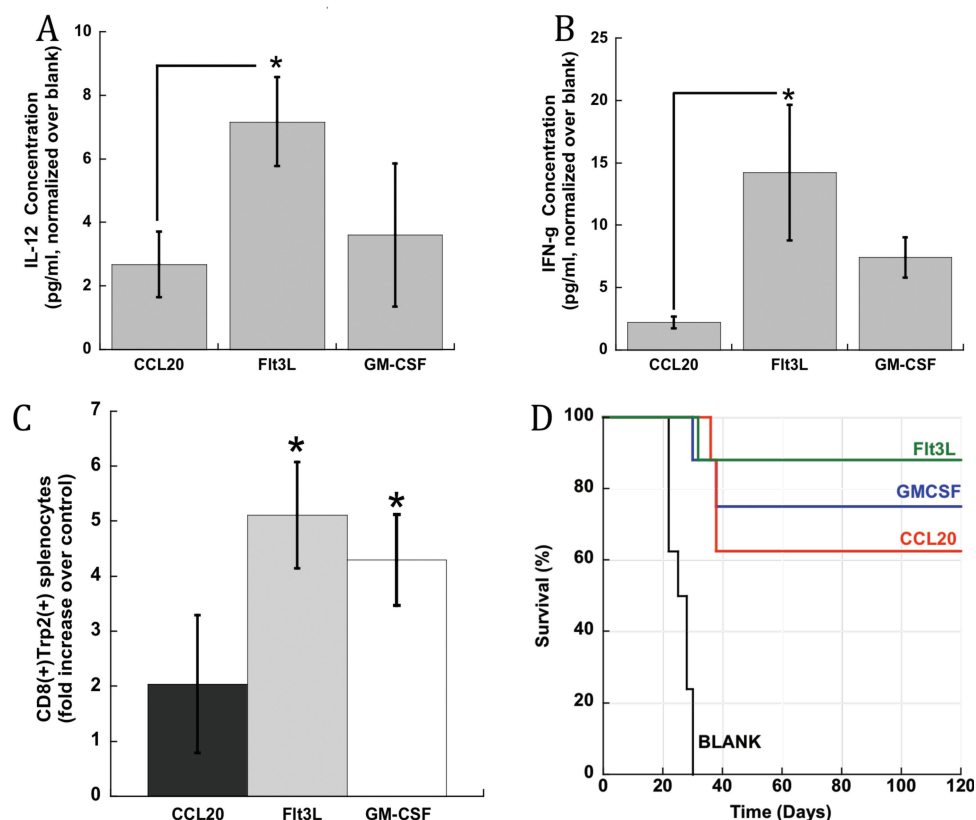
Figure 4. PLG vaccines generate immunoprotective cytokines, antigen-specific T cells, and cancer protection. Fold difference in local (A) IL-12 and (B) IFN-γ concentration after implantation of scaffolds loaded with B16-F10 tumor lysate, CpG-ODN in combination with CCL20, Flt3L, or GM-CSF. Concentrations were normalized to the value found in controls (matrices delivering lysate and CpG-ODN, no cytokines) (C) The total numbers of Trp2-specific CD8(+) T cells in spleens of vaccinated animals at Day 10 post-implantation. (D) The overall survival of mice bearing melanoma tumors, and treated with either CpG-ODN loaded matrices (Blank) or matrices loaded with CpG-ODN in combination with CCL20, Flt3L, and GM-CSF ($n = 8$). Values represent mean and standard deviations ($n = 5$). *$P < 0.05$, as compared to CCL20 loaded matrices.

systemic anti-melanoma CTLs and the local production of Th1 cytokines.

The anti-tumor efficacy of these vaccines were then tested in the poorly immunogenic, B16-F10 melanoma model. C57BL/6J mice were challenged with 10^5 tumor cells, and then vaccinated with PLG vaccines three days later. Animals treated with control scaffolds required euthanization after 30 days due to progressive disease. Importantly, PLG vaccines loaded with cytokines induced long-term tumor protection in a significant subset of animals (Figure 4D). GM-CSF, Flt3L and CCL20 presentation from PLG vaccines resulted in 88, 75 and 62% long-term survival rates (Figure 4D).

3. Discussion

Controlled mobilization and activation of DCs and DC precursors is of particular interest in the development of ex vivo DC based vaccines, and more generally, in the design of material systems that activate the immune system in vivo.[1,16,19] Here we report that polymers which mimic key aspects of microbial infection can effectively recruit DCs for cancer vaccination. PLG scaffolds engineered to release GM-CSF, Flt3L, and CCL20 led

to significant numbers of resident DCs, and the co-presentation of danger signals led to DC maturation. Even though all vaccine formulations were capable of inducing tumor protection in a therapeutic model of B16-F10 melanoma, GM-CSF and Flt3L vaccines produced more antigen specific CTLs, higher levels of Th1 priming cytokines, and greater survival rates when compared to CCL20 (Figure 4D). We, and others, have previously demonstrated that bolus delivery (naked cytokine or within microsphere depots) of DC chemoattractants in combination with tumor antigens and adjuvants failed to produce long-term survival in prophylactic cancer models.[1,17–20] In previous studies, we also demonstrated that PLG vaccine matrices releasing GM-CSF outperformed clinically tested, cell-based vaccines by enhancing the LN homing of activated DCs and long-term-survival in prophylactic B16 models.[17,18] These findings in combination with the results of this study suggest that the sustained release of chemotactic cytokines from macroporous vaccine structures are required to efficiently program DCs in situ to achieve vaccine efficacies superior to more traditional delivery methods.

Interestingly, while GM and Flt3L releasing PLG vaccines resulted in statistically similar T cell and anti-tumor responses, they had differential effects on DC recruitment and

activation. In vitro tests indicated that GM-CSF was the most potent chemotactic factor for cDCs (Figure 1). This finding was consistent with the ability of GM-CSF releasing matrices to recruit significantly more total DCs (~10^6, on par with ex vivo DC based protocols[1,16]) and activated DCs, in comparison to Flt3L scaffolds (Figures 2, 3). In contrast, and in agreement with other reports,[13,14] Flt3L vaccines led to more matrix- resident pDCs when combined with CpG-ODN danger signaling. pDCs are an important source of Th1 priming cytokines that amplify CTL responses, and increased pDC numbers likely contributed to the enhanced local production of IL-12 and IFNγ at the vaccine site. Further studies are required to confirm that pDCs are the primary source of these cytokines, or to identify other immune mechanisms that trigger the enhanced anti-tumor effect. Potentially, GM and Flt3L may be combined in material systems to exploit GM-CSF mediated activation of cDCs and Flt3L mediated generation of pDCs. These systems could be modified to optimize the DC network for cancer vaccination and immunotherapy.

Biomaterial particles are now being synthesized with adjuvant activity to complement their ability to control antigen or cytokine delivery for vaccination.[19–23] Nanoparticles have also been modified to target DC populations in vivo, and our findings suggest that pDCs, and their cDC counterparts should both be targeted to exploit their specialized abilities to mediate anti--tumor T cell responses.[19,21,24–27] In contrast to nanoparticle targeting systems, the polymer systems described in this report were designed to not only present infectious signals to recruit DCs, but also serve as a physical structure where DCs reside while they are activated. Interestingly, the processes that initiate and propagate adaptive immune responses are generally associated with lymphoid tissues, but have now been shown to also take place at the sites of infection,[28,29] where DCs and T cells both reside. The infection-mimicking materials described here may be used to study the mechanisms that act peripheral to lymphoid structures and that may underlie the generation of protective immunity.

While the systems described in this report demonstrated significant anti-tumor activity, they could be further optimized. Matrices could be fabricated from other, potentially, more inflammatory polymers to boost immune responses and DC mobilization. Although we analyzed the recruitment and activation of DCs, another important aspect of subsequent T cell priming by these cells is LN homing. The dispersement of DCs may be enhanced by incorporating different adjuvants into the material to activate migratory function. Other matrix properties, including degradation kinetics and porosity could be altered to promote further control over DC trafficking. In terms of clinical translation, implantation of the current system requires a surgical procedure, and the development of injectable or minimally invasive materials with similar porous frameworks would alleviate the need for surgical personnel and equipment and will be the subject of future studies. Finally, the cytokine release kinetics and dosing utilized in this report should be further scrutinized to examine their anti-tumor effect.

Altogether, these findings provide evidence that Flt3L, CCL20, and GM-CSF may be utilized in biomaterial systems to mimic infection-induced recruitment of DCs in situ. Infection-mimicking polymers demonstrate significant promise as therapeutic cancer vaccines. The methods described here may be adapted in the future to identify other cellular and molecular components that could be targeted for a variety of immunotherapeutic applications

4. Experimental Section

Mice: C57BL/6 mice (6–8-week-old female; Jackson Laboratories) were cared for in accordance with the American Association for the Accreditation of Laboratory Animal Care International regulations. Experiments were approved by the Harvard University Institutional Animal Care and use Committee.

Primary Cells (DCs) Isolation and Culture: A protocol developed by Lutz et al.[30] was adopted for generation of primary bone-marrow-derived dendritic cells (BMDCs). Briefly, bone marrow cells were flushed from the femurs of C57BL/6 mice and cultured in 100-mm bacteriological petri dishes (Falcon number 1029/Becton Dickinson). Cell culture medium RPMI-1640 (R10) (Sigma) was supplemented with 1% Penicillin–Streptomycin (Invitrogen), 2 mM l-Glutamine (Invitrogen), 50 μM 2-mercaptoethanol (Sigma) and 10% heat-inactivated fetal bovine serum (FBS, Invitrogen). At day 0, bone marrow leukocytes were seeded at 2×10^6 cells per 100-mm dish in 10 ml R10 medium containing 20 ng/mL granulocyte-macrophage colony-stimulating factor (GM-CSF) (Peprotech). At day 3 another 10 mL R10 medium containing 20 ng/mL GM-CSF was added to the plates. At days 6 and 8, half of the culture supernatant was collected and centrifuged, the cell pellet was resuspended in 10 mL fresh R10 containing 20 ng/mL GM-CSF, and placed back into the original plate. We used the non-adherent cell population in the culture supernatant between days 8 and 12 for all our experiments.

Transwell Migration Studies for Chemotaxis and Chemokinesis: Transwell migration studies for chemotaxis were performed by plating bone marrow derived dendritic cells in the top well of 6.5 mm transwell dishes (Costar, Cambridge, MA) with a pore size of 5 μm. The chemotactic effects of GM-CSF, Flt3L, and CCL20 on the migration of BMDCs were assessed by placing 10 ng/mL of recombinant murine GM-CSF, Flt3L or CCL20 (Peprotech, Rocky Hill, NJ) in the bottom wells and plating 3×10^5 DCs on the porous membrane of the top wells, For chemokinesis studies the concentration of cytokine in each compartment was kept at 10 ng/mL and 3×10^5 DCs were added to the top wells. The number of cells that migrated from the top well to the bottom well through the porous membrane was counted at the end of 12 h to quantify migration. Cells that had migrated to the bottom well were collected by treatment with 0.25% trypsin-0.03% ethylenediaminetetraacetic acid (EDTA, Invitrogen) and counted with a Z2 coulter counter (Beckman Coulter, Inc).

Matrix Fabrication: A 85:15, 120 kD copolymer of D,L-lactide and glycolide (PLG) (Alkermes, Cambridge, MA) was utilized in a gas-foaming process to form porous PLG matrices.[30] In brief, PLG microspheres encapsulating GM-CSF, Flt3L, or CCL20 were first made using standard double emulsion,[32] incorporating approximately 170 ng/mg of protein PLG microspheres. PLG microspheres were then mixed with 150 mg of the porogen, sucrose (sieved to a particle size between 250 μm and 425 μm), and compression molded. The resulting disc was allowed to equilibrate within a high-pressure CO_2 environment, and a rapid reduction in pressure causes the polymer particles to expand and fuse into an interconnected structure.[31] The sucrose was leached from the scaffolds by immersion in water yielding scaffolds that were 80–90% porous.

To incorporate tumor lysates into PLG scaffolds, biopsies of B16-F10 tumors that had grown subcutaneously in the backs of C57BL/6J mice (Jackson Laboratory, Bar Harbor Maine), were digested in collagenase (250 U/mL) (Worthington, Lakewood, NJ) and suspended at a concentration equivalent to 10^7 cells per ml after filtration through 40 μm cell strainers. The tumor cell suspension was subjected to 4 cycles of rapid freeze in liquid nitrogen and thaw (37 °C) and then

Materials
Views
www.MaterialsViews.com

ADVANCED
FUNCTIONAL
MATERIALS
www.afm-journal.de

FULL PAPER

centrifuged at 400 rpm for 10 min. The supernatant (1 mL) containing tumor lysates was collected, incubated with the PLG microspheres and lyophilized and the resulting mixture was used to make PLG scaffold-based cancer vaccines.

To incorporate CpG-ODNs into PLG scaffolds, CpG-ODN 1826, 5′-tcc atg acg ttc ctg acg tt-3′, (Invivogen, San Diego, CA) was first condensed with poly(ethylenimine) (PEI, Mn ~60 000, Sigma Aldrich) molecules by dropping ODN-1826 solutions into PEI solution, while vortexing the mixture.[16] The charge ratio between PEI and CpG-ODN (NH3+:PO4−) was kept constant at 7 during condensation.

The condensate solutions were then vortexed with 60 μL of 50% (wt/vol) sucrose solution, lyophilized and mixed with dry sucrose to a final weight of 150 mg. The sucrose containing approximately 100 μg PEI-CpG-ODN condensate was then mixed with blank, GM-CSF and/or tumor lysate loaded PLG microspheres to make PLG cancer vaccines.

In situ Identification of DCs and T cells: GM-CSF loaded PLG matrices containing approximately 3 μg of GM-CSF, Flt3L, or CCL20 in combination with 100 μg of CpG-ODN were implanted into subcutaneous pockets on the back of 7–9 week old female C57BL/6J mice. To analyze DC recruitment by FACS analysis, scaffolds were excised and the ingrown tissue was digested into single cell suspensions using a collagenase solution (Worthingtion, 250 U/ml) that was agitated at 37 °C for 45 min. The cell suspensions were then poured through a 40 μm cell strainer to isolate cells from scaffold particles and the cells were pelleted and washed with cold PBS and counted using a Z2 coulter counter (Beckman Coulter). To assess, DC infiltration and activation, subsets of the total cell population isolated from PLG matrices were then stained with primary antibodies (BD Pharmingen, San Diego, CA) conjugated to fluorescent markers to allow for analysis by flow cytometry. APC-conjugated CD11c (dendritic cell marker), FITC-conjugated MHCII and PE-conjugated CD86 (B7, costimulatory molecule) stains were conducted for DC recruitment and activation analysis. To delineate the presence of the plasmacytoid DC subset, cells were also stained with APC-conjugated CD11c and PE-conjugated PDCA-1 (plasmacytoid DC marker). Cells were gated according to single positive FITC, APC and PE stainings using isotype controls. The percentage of cells staining positive for each surface antigen was recorded.

For the immunostaining of DC infiltrates in paraffin sections of scaffolds, samples were prepared and re-hydrated according to standard procedures.[33] Antigen retrieval was done with citrate buffer in a pressurized cooker (10 mM Sodium Citrate, 0.05% Tween 20, pH 6.0, for 5 min in 950C). After brief washes with PBST buffer (0.01% Tween-20), samples were blocked with 5% goat serum in staining buffer (5%BSA, 2% Fetal Bovine Serum in PBST, pH 7.4) for 1 hour in ambient temperature. Anti-CD11c Armenian Hamster IgG (20 mg/mL, Abcam, Cambridge, MA) was diluted in staining buffer and allowed to bind overnight at 40C in a humidified chamber. After washing 3 times with PBST, Alexa594 Goat anti-Hamster (5 mg/mL, Life Technologies, Grand Island, NY) secondary IgG was diluted in staining buffer and applied for 1 h at RT. After three washes with PBS, samples were air-dried and mounted with ProLong Gold Antifade reagent with DAPI for nuclear staining (Life Technologies, Grand Island, NY). Confocal tile scans were obtained and processed with Zeiss LSM 710 laser-scanning microscope and bundled software (Zeiss, Thornwood, NY).

Tumor Growth Assays, Protective Cytokines and Trp2 Pentamer Analysis: PLG scaffolds containing B16-F10 melanoma tumor lysates, 100 μg CpG-ODN in combination with 3μg GM-CSF, Flt3L or CCL20 were implanted subcutaneously into the lower left flank of C57BL/6J mice to act as cancer vaccines. To assess PLG vaccine efficacy in the therapeutic setting, C57/BL6J mice were challenged with a subcutaneous injection of 1×10^5 B16-F10 melanoma cells (ATCC, Manassas, NJ) in the back of the neck, and 3 days after tumor challenge PLG vaccines were implanted subcutaneously into the lower left flank. Animals were monitored for the onset of tumor growth (approximately 1mm3) and sacrificed for humane reasons when tumors grew to 20–25 mm (longest diameter).

To determine the in vivo IL-12p70 and IFN-γ concentration at the matrix implant site, adjacent tissue was excised and digested with tissue protein extraction reagent at Day 10 after implantation (Pierce).

After centrifugation, the concentrations of IL-12 and IFN-γ, in the supernatant were then analyzed with ELISA (R&D systems), according to the manufacturers instructions. To determine the generation of TRP-2-specific cytotoxic T lymphocytes, single cell suspensions were prepared at Day 10 from the spleens of mice immunized with PLG vaccines. These cells were initially stained with PE-H-2Kb/TRP2 pentamers (Sigma Aldrich), and subsequently stained with FITC-anti-CD8 and PE-CY7 CD3 mAb (mAb (BD Pharmingen, San Diego) before being analyzed using flow cytometry.

Acknowledgements

[1] E. Gilboa, *J. Clin. Invest.* **2007**, *117*, 1195–1203.
[2] Y. J. Liu, *Cell* **2001**, *106*, 259–262.
[3] G. Jego, K. A. Palucka, J. P. Blank, P. Chalouni, J. Banchereau, *Immunity* **2003**, *19*, 225–234.
[4] G. J. Randolph, J. Ochando, S. Partida-Sanchez, *Annu. Rev. Immunol.* **2008**, *26*, 293–316.
[5] J. Banchereau, R. M. Steinman, *Nature* **1998**, *392*, 245–252.
[6] D. M. Klinman, *Nat. Rev. Immunol.* **2004**, *4*, 249.
[7] A. Lanzavecchia, F. Sallusto, *Cell* **2001**, *106*, 263–266.
[8] J. Hamilton, G. Anderson, *Growth Factors* **2004**, *22*, 225–231.
[9] J. Hamilton, *Trends Immunol.* **2002**, 403–408.
[10] S. He, Q. Cao, H. Yoneyama, H. Ge, Y. Zhang, *J. Leukoc. Biol.* **2008**, *84*, 1549.
[11] M. C. Dieu, B. Vanbervliet, A. Vicari, J. M. Bridon, E. Oldham, S. Ait-Yahia, F. Briere, A. Ziotnik, S. Lebecque, C. Caux, *J. Exp. Med.* **1998**, *188*, 373.
[12] K. Holger, M. Merad, A. Cozzio, I. Weissman, M. Manzi, *J. Exp. Med.* **2003**, *198*, 305–313.
[13] N. Onal, A. Obata-Onai, M. A. Schmid, M. G. Manz, *Ann. NY Acad. Sci.* **2007**, *1106*, 253.
[14] N. Mach, S. Gillessen, S. B. Wilson, C. Sheehan, M. Mihm, G. Dranoff, *Cancer Res.* **2000**, *60*, 3239.
[15] S. A. Rosenberg, J. C. Yang, N. P. Restifo, *Nat. Med.* **2004**, *10*, 909–915.
[16] M. Hansen, G. M. Jjorto, M. Donia, O. Met, N. B. Larsen, M. H. Andersen, P. Thos Straten, I. M. Svane, *Vaccine* **2012**, *4*, 639–646.
[17] O. A. Ali, N. Huebsch, L. Cao, G. Dranoff, D. J. Mooney, *Nat. Mater.* **2009**, *2*, 151.
[18] O. A. Ali, D. Emerich, G. Dranoff, D. J. Mooney, *Sci. Transl. Med.* **2009**, *1*, 8–19.
[19] O. A. Ali, D. J. Mooney, *Curr. Top. Microbiol. Immunol.* **2011**, *344*, 279.
[20] N. K. Egilmez, Y. S. Jong, M. S. Sabel, J. S. Jacob, E. Mathiowitz, R. B. Bankert, *Cancer Res.* **2000**, *60*, 3832–3837.
[21] J. A. Hubbell, S. N. Thomas, M. A. Swartz, *Nature* **2009**, *462*, 449–460.
[22] S. R. Little, D. M. Lynn, Q. Ge, *Proc. Natl. Acad. Sci. USA* **2004**, *101*, 9534–9539.
[23] N. Bennewitz, J. E. Babensee, *Biomaterials* **2005**, *26*, 2991–2999.

FULL PAPER

[24] S. T. Reddy, A. J. Van Der Vlies, E. Simeon, *Nat. Biotechnol.* **2007**, *2*, 1159–1164.

[25] C. Oussoren, G. Storm, *Adv. Drug Deliv. Rev.* **2001**, *50*, 143–156.

[26] S. R. Little, D. M. Lynn, Q. Ge, D. G. Anderson, S.V. Puram, J. Chen, H. N. Eisen, R. Langer, *Proc. Natl. Acad. Sci. USA* **2004**, *101*, 9534–9539.

[27] C. L. Van Broekhoven, C. R. Parish, C. Demangel, *Cancer Res.* **2004**, *64*, 4357-4365.

[28] G. Fousteri, A. Dave, A. Juedes, T. Juntti, B. Morin, L. Togher, D. L. Farber, M. Von Herrath, *PLOS One* **2011**, 1.

[29] L. M. Wakim, J. Waithman, N. Van Rooijen, W. R. Heath, F. R. Carbone, *Science* **2008**, *319*, 198–202.

[30] M. B. Lutz, N. Kukutsch, A. L. J. Ogilvie, S. Rossner, F. Koch, N. Romani, *J. Immunol. Methods.* **1999**, *223*, 77–92.

[31] L. D. Harris, B. S. Kim, D. J. Mooney, *J. Biomed. Mater. Res.* **1998**, *42*, 396–402.

[32] S. Cohen, T. Yoshioka, M. Lucarelli, L. H. Hwang, R. Langer, *Pharm. Res.* **1991**, *8*, 713–720.

[33] S. R. Shi, Y. Shi, C. R. Taylor, *J. Histochem. Cytochem.* **2011**, *59* 13–32.